The Fusion Kinetics of Influenza Hemagglutinin Expressing Cells to Planar Bilayer Membranes Is Affected by HA Density and Host Cell Surface

GRIGORY B. MELIKYAN, WALTER D. NILES, and FREDRIC S. COHEN

From the Department of Molecular Biophysics and Physiology, Rush Medical College, Chicago, Illinois 60612

ABSTRACT Time-resolved admittance measurements were used to follow formation of individual fusion pores connecting influenza virus hemagglutinin (HA)-expressing cells to planar bilayer membranes. By measuring in-phase, out-of-phase, and dc components of currents, pore conductances were resolved with millisecond time resolution. Fusion pores developed in stages, from small pores flickering open and closed, to small successful pores that remained open until enlarging their lumens to sizes greater than those of viral nucleocapsids. The kinetics of fusion and the properties of fusion pores were studied as functions of density of the fusion protein HA. The consequences of treating cell surfaces with proteases that do not affect HA were also investigated. Fusion kinetics were described by waiting time distributions from triggering fusion, by lowering pH, to the moment of pore formation. The kinetics of pore formation became faster as the density of active HA was made greater or when cell surface proteins were extensively cleaved with proteases. In accord with this faster kinetics, the intervals between transient pore openings within the flickering stage were shorter for higher HA density and more extensive cell surface treatment. Whereas the kinetics of fusion depended on HA density, the lifetimes of open fusion pores were independent of HA density. However, the lifetimes of open pores were affected by the proteolytic treatment of the cells. Faster fusion kinetics correlated with shorter pore openings. We conclude that the density of fusion protein strongly affects the kinetics of fusion pore formation, but that once formed, pore evolution is not under control of fusion proteins but rather under the influence of mechanical forces, such as membrane bending and tension.

INTRODUCTION

Biological membrane fusion is a protein-mediated event, so the proteins responsible have been sought and candidates cloned (White, 1992; Söllner and Rothman, 1994; Ferro-Novick and Jahn, 1994). Only the fusion proteins of viruses, however,

Address correspondence to Dr. Fredric S. Cohen, Department of Molecular Biophysics and Physiology, 1653 West Congress Parkway, Chicago, IL 60612.

J. GEN. PHYSIOL. © The Rockefeller University Press · 0022-1295/95/11/783/20 $2.00
Volume 106 November 1995 783–802

have so far been unambiguously identified. Hemagglutinin (HA) of influenza virus, located in the viral envelope, is responsible for both binding and fusion to the host membrane (White, Helenius, and Gething 1982). The nonfusogenic, neutral-pH form of the ectodomain of HA and several mutants have been crystallized and their structures determined to 3 Å (Wilson, Skehel, and Wiley, 1981). The HA glycoprotein is assembled from three identical monomers, each synthesized as a single polypeptide chain, HA0. HA0 is not fusogenic. Only when the monomers are proteolytically cleaved to HA1-HA2 subunits linked by a disulfide bond do the trimers exhibit fusogenic activity (Wiley and Skehel, 1987). When exposed to low pH, the active HA undergoes substantial conformational changes (Skehel, Bayley, Brown, Martin, Waterfield, White, Wilson, and Wiley, 1982; Yewdell, Gerhard, and Bachi, 1983; Doms, Helenius, and White, 1985; White and Wilson, 1987; Stegmann, White, and Helenius, 1990; Bullough, Hughson, Skehel, and Wiley, 1994), leading, in a still unknown manner, to fusion pore formation (Spruce, Iwata, White, and Almers, 1989; Spruce, Iwata, and Almers, 1991; Zimmerberg, Vogel, and Chernomordik, 1993; Zimmerberg, Blumenthal, Sarkar, Curran, and Morris, 1994).

A powerful means of combining molecular biology to functional study is to express mutated HA on cell surfaces (Doyle, Roth, Sambrook, and Gething, 1985; Gething, Doms, York, and White, 1986; Nobusawa and Nakajima, 1988; Godley, Pfeifer, Steinhauser, Ely, Shaw, Kaufmann, Suchanek, Pabo, Skehel, Wiley, and Wharton, 1992; Kemble, Henis, and White, 1993). Thus, much effort has been devoted to studying fusion of HA-expressing cells to other cells (White et al., 1982; Doxsey, Sambrook, Helenius, and White, 1985; Sambrook, Rodgers, White, and Gething, 1985; Morris, Sarkar, White, and Blumenthal, 1989; Sarkar, Morris, Eidelman, Zimmerberg, and Blumenthal, 1989; Spruce et al., 1989; Clague, Schoch, and Blumenthal, 1991; Kaplan, Zimmerberg, Puri, Sarkar, and Blumenthal, 1991) or to lipid bilayers (van Meer and Simons, 1983; Ellens, Bentz, Mason, Zhang, and White, 1990; Melikyan, Niles, Peeples, and Cohen, 1993*a*). As with intact virus, in the cell HA expression systems fusion is pH and temperature dependent. However, the density of HA is higher in virus than in cells (Ruigrok, Andree, Hooft van Huysduynen, and Mellema, 1984; Ellens et al., 1990) and the envelopes of virus are less complex than are cell surfaces. These distinctions may be important since both the delay from acidification to fusion decreases (Clague et al., 1991) and the extent of fusion increases (Ellens et al., 1990) with HA density. The effects of the host cell membrane on fusion have not been systematically studied, but HA-expressing cells have been routinely treated with neuraminidase to increase the extent and rates of fusion (Ellens, Doxsey, Glenn, and White, 1989; Sarkar et al., 1989; Puri, Booy, Doms, White, and Blumenthal, 1990; Kemble, Danieli, and White, 1994). We therefore explored the effects of the density of HA on fusion by using two cell lines, HAb2 and GP4f, of known density (Ellens et al., 1990) or by varying the extent HA0 was proteolytically cleaved to its fusogenic form in HAb2 cell membranes (Clague et al., 1991). We also determined how variation in the proteolytic treatment of cell surfaces of HA-expressing cells affected fusion kinetics.

We accomplished this by using time-resolved admittance measurements, with high sensitivity and high time resolution, to monitor the kinetics of fusion pore formation between HA-expressing cells and planar lipid bilayer membranes. The ki-

netics of fusion pore formation was quite sensitive to both active HA density and proteolytic treatment. In contrast, the lifetimes of small transient pores did not depend on HA density, but were shorter for more extensive cell surface proteolysis. We conclude that while HAs are required for fusion pore formation, once the pores have formed their evolution does not depend on the density of HA, but rather depends predominantly on the balance of mechanical factors in the fusing membranes.

MATERIALS AND METHODS

Cell Culture

Two subclones from the same line of stably transfected NIH-3T3 fibroblasts, HAb2 (Doxsey et al., 1985) and GP4f (Ellens et al., 1990), expressing the A/Japan/305/57 strain of influenza virus HA were provided by J. M. White (University of Virginia, Charlottesville, VA) (see also Sambrook et al., 1985). Cells were maintained in DMEM medium (GIBCO BRL, Gaithersburg, MD) supplemented with 10% fetal bovine serum, 110 U/ml penicillin, 100 μg/ml streptomycin in 5% CO_2, 37°C, and released for passage from plastic culture dishes by incubating in phosphate buffered saline (PBS) with 0.5 mg/ml EDTA and 0.5 mg/ml EGTA for 12–15 min at 37°C.

Differential Cleavage of HA

For fusion experiments, cells were lifted from culture dishes and their surfaces enzymatically treated. The expressed HA0 was always activated by cleavage with trypsin. Several protocols were followed, each denoted by a symbol of the form X/Y. X signifies the extent to which HA0 was cleaved: full (F), extensive but not full (E), or low (L). Y signifies how the cell surface was enzymatically affected: surfaces could be treated with either high concentrations of trypsin (T), chymotrypsin (C), or a hyaluronidase-collagenase mixture (H), or could be untreated (U). The extents of cleavage were established by labeling cells with [^{35}S]methionine and immunoprecipitating cell lysates (Morrison, McQuain, and McGinnes, 1991) with sera against Japan/57 virus (provided by J. M. White). The precipitates were separated by SDS-PAGE under reducing conditions and the HA2 band on the autoradiogram was analyzed by densitometry.

Cell Treatment

The four protocols were: (*a*) Cells were incubated with 0.5 mg/ml trypsin (TPCK treated, Sigma Chemical Co., St. Louis, MO), 0.2 mg/ml EDTA in PBS for 6 min at 37°C. The reaction was stopped by adding an excess of soybean trypsin inhibitor (STI; Sigma Chemical Co.). This "high trypsin" cleaved all HA0 and enzymatically affected the cell surfaces. These cells are thus denoted F/T. (*b*) In a milder trypsin treatment ("low trypsin") cells were lifted with 0.5 mg/ml EDTA/EGTA in PBS (see above) and incubated with 1 μg/ml trypsin in PBS at room temperature. Either 2.5 or 12 min later, trypsin activity was suppressed by adding an excess of STI. HA0 is particularly susceptible to trypsin at a well-defined site (Doms et al., 1985). The low concentration of trypsin should affect the other proteins to a much lower degree than the high concentration of proteases used in other treatments. We consider these cells as effectively "untreated." We did not treat cells with low trypsin for longer than 12 min to minimize proteolysis of surface proteins. The HA2 band on the autoradiogram (not shown) was about two times less intense for the 2.5-min exposure than for the 12-min exposure, which in turn was only somewhat less intense than for fully cleaved HA (F/T cells). The HA2 band was absent when cells were not treated with trypsin, demonstrating that tryspin was required for cleavage of HA0. We refer to cells treated with the low trypsin for 12 min as E/U; cells treated for 2.5 min are denoted as L/U. (*c*) Cells were lifted and surfaces treated

by incubating with 0.5 mg/ml chymotrypsin (TLCK treated; Sigma Chemical Co.), 5 μg/ml STI, 0.2 mg/ml EDTA in PBS for 6 min at 37°C. The HA0 was then cleaved with a 12-min incubation with 1 μg/ml trypsin in PBS. Chymotrypsin activity was inhibited by adding DMEM with 10% fetal bovine serum. These cells are denoted by E/C. (*d*) Cells were lifted with EDTA/EGTA in PBS solution and specific proteolysis of cell surface proteins was achieved by incubating cells with 0.3 mg/ml hyaluronidase (type IV-S from bovine testes; Sigma Chemical Co.) and 0.2% collagenase P (Boehringer Mannheim Corp., Indianapolis, IN) in PBS for 20 min at 37°C. Cells were then washed twice with PBS and incubated with 1 μg/ml trypsin in PBS for 12 min. These cells are denoted E/H.

Fusion efficiency was increased in all four cases by incubating cells with 0.5 mg/ml neuraminidase (from *Clostridium perfringence*, type V; Sigma Chemical Co.) in PBS for 7 min at 37°C (Ellens et al., 1990). After all protease/sialidase treatments, cells were washed three times, concentrated, and stored in PBS on ice and used for experiments within 6 h.

For convenience, we summarize the nomenclature. F/T: HA0 fully cleaved, surfaces exposed to high concentration of trypsin. E/C: extensive cleavage of HA0, surfaces treated with a high concentration of chymotrypsin. E/H: extensive cleavage of HA0, surfaces processed by hyaluronidase/collagenase. E/U: extensive cleavage of HA0, surfaces untreated. L/U: low cleavage of HA0, surfaces untreated.

Planar Membrane Formation and Cell-Bilayer Fusion

Solvent-free horizontal lipid bilayers were formed from a solution of dioleoylphosphatidylcholine/bovine brain phosphatidylethanolamine (Avanti Polar Lipids, Inc., Pelham, AL) 2:1 (wt/wt) with 5 mol% of brain gangliosides G_{D1a}/G_{T1b} 1:1 wt/wt (Sigma Chemical Co.) in squalene (Aldrich Chemical Co., Milwaukee, WI) that had been passed through an alumina column. The gangliosides functioned as binding receptors for HA (Suzuki, Nagao, Kato, Matsumoto, Nerome, Nakajima, and Nobusawa, 1986). Planar bilayers were formed in a 150-μm diam hole in a black Teflon film with a brush technique and were bathed in symmetrical 140 mM NaCl, 2.5 mM KCl, 5 mM $MgCl_2$, 2 mM $CaCl_2$, 1 mM Pipes, pH = 6.3 maintained at 35–37°C. Membrane formation and cell contact with the bilayer were observed with an inverted microscope (Nikon Diaphot, Garden City, NY).

Small amounts (~10 μl) of a concentrated cell suspension (~10^7 cells/ml) in PBS were added above the planar membrane with a micropipette. The cells spontaneously sedimented and within 30-50 s 15–25 of the cells rested upon the membrane. The remainder of the cells came to rest on the teflon partition and never achieved contact with the bilayer. 4–5 min after the cells established contact with the lipid membrane, fusion was triggered by lowering the pH of the top, cell-containing, solution to 4.9 by injecting 25 μl of concentrated isotonic succinate buffer directly over the bilayer. Control experiments measuring conductance of the planar bilayer in the presence of the proton carrier, FCCP, established that acidification occurred within 1–3 s (Melikyan et al., 1993*a*).

Time Resolved Admittance Measurement

Cell-bilayer fusion was monitored by changes in bilayer admittance. The bilayer was voltage-clamped and a sine wave, superimposed on a holding potential of 20 mV, was applied as a command voltage to the bottom solution bathing the membrane. The in-phase (Y_0), out-of-phase (Y_{90}), and dc (Y_{dc}) components of admittance were calculated on-line with a software-based phase detector (Joshi and Fernandez, 1988). These components of the admittance yielded time-resolved values of the fusion pore conductance (g) in series with the parallel combination of the cell membrane conductance (G_c) and capacitance (C_c) according to the equations (Lindau and Neher, 1988; Melikyan, Niles, Ratinov, Karhanek, Zimmerberg, and Cohen, 1995): $g = a/b$; $G_c = aY_{dc}/(b^2 + Y_{90}^2)$; $C_c = a^2/[\omega Y_{90}(b^2 + Y_{90}^2)]$, where $a = Y_0^2 + Y_{90}^2 - Y_0 Y_{dc}$, $b = Y_0 - Y_{dc}$, and $\omega = 2\pi f$ where

f is the frequency of the applied sine wave voltage. For display, Y_0 and Y_{90} currents were converted into their natural units of conductance (nS). Data were stored on hard disk and analyzed off-line.

The openings of pores were timed by noting when $Y_0 - Y_{dc}$ deviated from zero. When current flowed through small fusion pores, $Y_0 \approx g$ ($g << \omega C_c$) and $Y_{dc} = gG_c/(g + G_c)$, and hence $Y_0 > Y_{dc}$ (provided G_c is not much larger than g). In contrast, for current through the bilayer, $Y_0 = Y_{dc} = G_m$. Therefore, any changes in Y_0 after subtracting Y_{dc} had to be due to pore formation or closure, and not due to increases in G_m.

Data Analysis

We obtained the kinetics of fusion on the level of single events by producing waiting time distributions for formation of the first fusion pore, t_Q. The waiting time from the trigger (acidification) to the opening of the first fusion pore was measured (see Fig. 1). The distribution of waiting times yields the probability $P(t)$ that pores have not formed by time t. Equivalently, $P(t) = N(t)/N(0)$ where $N(t)$ is the number of pores that have not yet formed by time t and $N(0)$ is the total number of pores (i.e., no pore has formed at time = 0). Clearly, the waiting time distribution decays from $P(t = 0) = N(t = 0)/N(0) = 1$. We fit the last 50% of the points of the waiting time distributions with single exponentials (Fig. 2 *A*, *solid lines*) and extrapolated to $P(t) = 1$. The extrapolated times were taken as the delay times, t_D, and the final slopes of the distributions plotted semilogarithmically were denoted, k_F. t_D and k_F are summarized for the various treatments in Table I. t_D are analogous to delays measured in homogeneous population studies (Clague et al., 1991; Bentz, 1992) and k_F yields the rate limiting step. Waiting time distributions are simply (1 − [cumulative probability density functions]). While either waiting time or cumulative probability distributions can be used to evaluate kinetics, delays and final slopes are more apparent from waiting time distributions.

It is uncertain whether the multiple flickers are due to several distinct transient pores or the same pore repetitively opening and closing. The events numbered 1 through 5 on the g trace (Fig. 1, *top*) could arise from a single pore opening and closing five times, or each event could represent a different pore from either the same cell or different cells adhered to the planar bilayer. If the same pore were flickering, the time course of fusion would be obtained from the distribution of times from acidification to the first flicker, t_Q (Fig. 1, *bottom, triangles*). If different pores were flickering, the time course of fusion would be determined from the distribution of times from the moment fusion was triggered until the moment each flickering pore opened, t_F (Fig. 1, *circles*). The flickering pores could also be viewed as incomplete fusion, in which case the waiting times from acidification to fully opened terminal stage pores, t_T (Fig. 2, *squares*), determined by a stepwise increase in Y_{90} (Melikyan, Niles, and Cohen, 1993*b*), would yield the kinetics of fusion. Because the times that pores were in the flickering stage and remained irreversibly open before full enlargement were short compared to t_Q, the waiting times t_F and t_T were only marginally longer than t_Q. In fact, these three distributions were not significantly different. We used the t_Q distribution to evaluate the kinetics of fusion because the opening of the first pore could always be unambiguously determined and because the relation of subsequent flickers to the first has not been settled.

Open times of individual flickering pores, t_o, were determined and plotted as open lifetime distributions (i.e., waiting times for closure). These are displayed as $N(t)/N(0)$ where $N(t)$ is the number of pores still open at time t after opening and $N(0)$ is the total number of pores included in the distribution (i.e., all pores are open at $t = 0$). The interflicker intervals, t_i, were obtained as the distributions of waiting times between successive openings of transient fusion pores.

The *S* stage is initiated when a fusion pore irreversibly opens and terminates when it rapidly enlarges into the fully enlarged terminal *T* stage. Because these *S* stage pores dilate to sizes sufficiently large to allow release of viral nucleocapsids, we refer to them as "successful." The times pores spent in the successful, *S*, stage (t_S) were measured and plotted as waiting time distributions

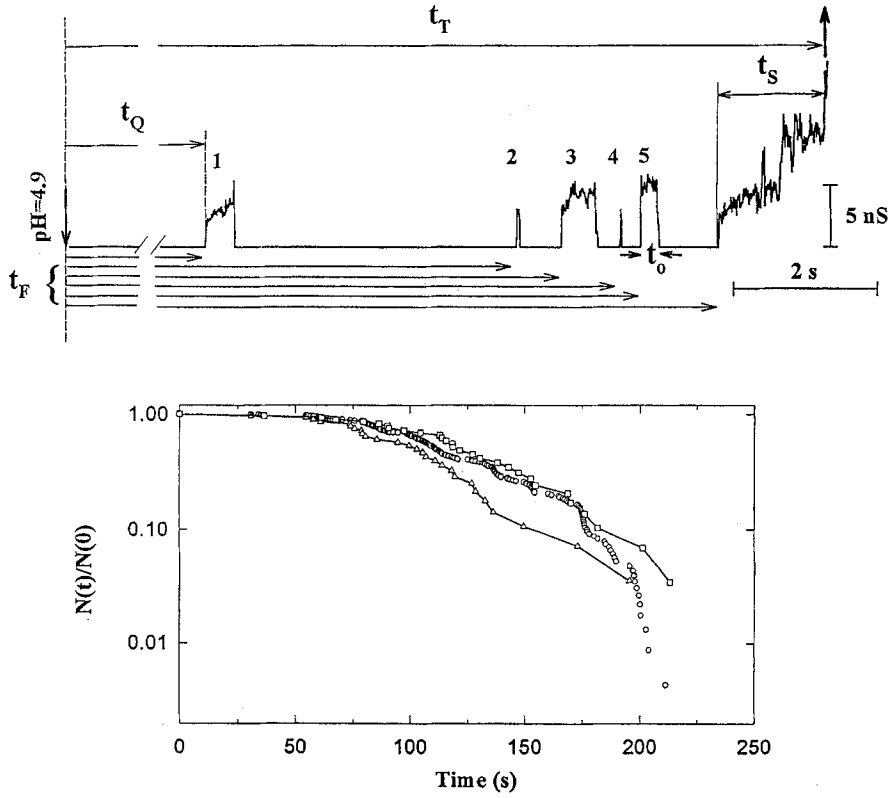

FIGURE 1. (*Top*) The conductance of fusion pores develops in stages. Fusion pore conductances were calculated as described in Materials and Methods. The times from acidification to pH 4.9 (marked by downward arrow, time = 0) to the first fusion pore, t_Q, to each transient pore opening, t_F, and to the terminal fully open pore, t_T are shown. The time omitted within t_Q by the breakmark was 96 s. Each flicker is numbered (1–5) and t_o for flicker 5 is indicated. The flicker and stepwise changes in conductance for this particular successful pore of duration t_S may be due to either the formation of a second pore or stepwise conductance changes of a pore previously formed. The arrow up marks the moment the pore enlarged abruptly to ~1 μS. (*Bottom*) Waiting time distributions for the opening of the first pore between F/T cells and planar membranes (t_Q, *triangles*) and for all flickers (t_F, *circles*), as well as for a pore to completely dilate into the *T* stage (t_T, *squares*). The normalized number of pores that have not formed by time t after acidification is plotted as a function of t. Experimental points are connected by solid lines to aid visual clarity. All three waiting time distributions are statistically identical by the Kolmogorov-Smirnov test ($p > 0.05$).

(Fig. 1). Also, the times that all pores (transient and successful) remained open before enlargement to the *T* stage were summed for each experiment and plotted as total open time distributions, T_{os}. For example, in Fig. 1, T_{os} is the sum of the lifetimes for each of the five individual flickers (t_o) and the lifetime of the successful pore (t_S) before complete enlargement.

Differences between distributions for various experimental protocols were evaluated by the nonparametric two-sample Kolmogorov-Smirnov test. Our criterion for distributions to be indistinguishable was that the attained level of significance be $p > 0.05$. The actual attained levels are given in the appropriate figure legends.

RESULTS

Cell-bilayer Fusion Evolved in Stages

After 15–25 cells adhered to the horizontal planar bilayer, we triggered fusion by lowering the pH of the solution above the membrane (Fig. 1, *top*, pH = 4.9, *downward arrow*). After an electrically quiescent stage (*Q*), fusion pores with typical conductances on the order of 2–5 nS were observed to repetitively flicker open and closed. Subsequently, a successful pore was observed to open (*S* stage). After variable times in this stage, pores expanded into the terminal *T* stage with an instantaneous (faster than we could resolve) rise in g to ~1 μS (not shown). Pores were labeled successful, a posteriori, if they enlarged into *T* stage pores. Control experiments established that the admittance increases attributed to fusion were absolutely dependent on active, cleaved HA. Cells lifted from dishes with PBS solutions containing EDTA/EGTA or chymotrypsin/EDTA, expressing only uncleaved HA0 (Clague et al., 1991; J. White, personal communication), never caused the fusion-associated admittance changes for as long as tested (40–45 min).

Under some conditions, complete fusion was not always detected with as many as 15–25 cells adhered to the horizontal bilayer. Complete pore enlargement was routinely seen when the HA0 on HAb2 cells was extensively cleaved and the cell surface enzymatically treated (i.e., F/T, E/C and E/H cells). However, F/T GP4f cells, with their lower HA density than HAb2 cells, did not exhibit T stage pores in ~40% of the experiments, and E/U HAb2 cells with untreated cell surfaces did not express T stage pores for ~25% of the membranes. Full enlargement of fusion pores was not observed in ~50% of the experiments with L/U HAb2 cells. In contrast, transient fusion pore formation was recorded in almost all experiments regardless of the proteolytic treatment.

Soon after the first pore dilated into the *T* stage, Y_0 and Y_{dc} tended to rise monotonically and in parallel. The current usually saturated the amplifier in ~15 s. Because these increases in current temporally correlated with pores opening to the large conductance of ~1 μS, we surmise that they were due to the fused cell membrane becoming progressively leaky. Obviously, subsequent pores (connecting other cells to the planar membrane) fully enlarging into the *T* stage could be followed for only the brief time before amplifier saturation. Subsequent pore flickering and pore enlargement could not be measured after this point. As a result, the efficiency of fusion, defined as the percentage of adhered cells that fused (with full enlargement of the fusion pore), could not be reliably quantified by electrical means. We wanted to study the entire evolution of pore development, from flickering through full enlargement. Therefore, we tolerated the ambiguities resulting from adhering many cells to the planar membrane to maximize our chance of obtaining complete, T stage, fusion.

Higher HA Density Speeds Pore Formation but Does Not Affect the Lifetimes of Transient and Successful Pores

Waiting time distributions from acidification to the first transient pore opening (t_Q) were used to characterize fusion. GP4f cells (Fig. 2 *A*, *open circles*) have 1.9

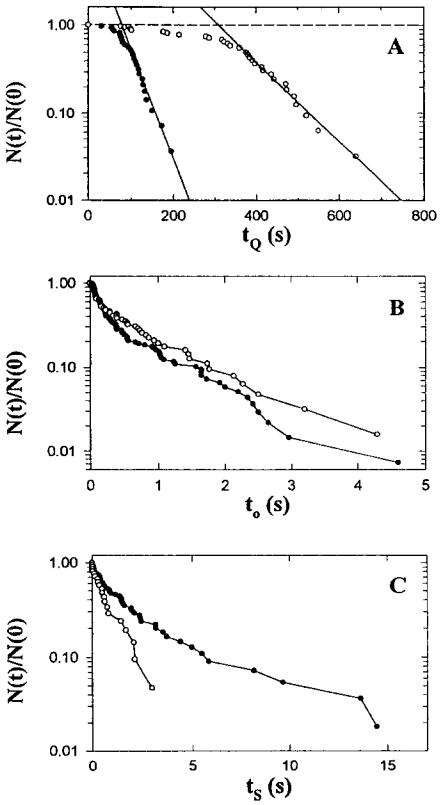

FIGURE 2. Fusion kinetics of F/T HAb2 (*filled circles*) and F/T GP4f (*open circles*) cells. (*A*) Waiting time distributions, t_Q. Solid lines were obtained by fitting the last 50% of the points with single exponentials. Extrapolating these curves to $N(t)/N(0) = 1$ gave the delay times, t_D (see Table I). (*B*) The open times of transient fusion pores t_o plotted as waiting time distributions until closure. The distributions of the two cell lines were indistinguishable ($p > 0.1$). (*C*) The waiting time distributions from formation until dilation into the *T* stage for successful pores (t_S) were not statistically different for the two cell lines ($p > 0.05$).

times lower density of HA than HAb2 cells (Ellens et al.,1990). F/T GP4f cells fused more slowly than similarly treated F/T HAb2 cells (*filled circles*). The delay times, t_D, were 310 and 79 s for GP4f and F/T HAb2 cells, respectively (see Table I). The final slopes of exponentials fitted to the last 50% of points, k_F, were 0.011 s^{-1} (GP4f) and 0.029 s^{-1} (HAb2). Thus, the delays until fusion were shorter and final slopes of the waiting time distributions were greater with a higher density of HA.

We characterized both flickering and successful fusion pores by their open time distributions, t_o and t_S, respectively. The t_o distributions for F/T HAb2 (Fig. 2 *B*, *filled circles*) and GP4f (*open circles*) cells were statistically identical, despite the higher HA density for HAb2 cells. The t_S distributions (Fig. 2 *C*) were also statisti-

TABLE I

The Delay Times (t_D) and Final Slopes (k_F) of the Waiting Time Distributions for Formation of the First Fusion Pore

Treatment Parameters	F/T HAb2	E/C HAb2	E/H HAb2	E/U HAb2	L/U HAb2	F/T GP4f
t_D(s)	79.0	23.6	28.1	119.0	266.9	310.4
k_F(s^{-1})	0.029	0.029	0.026	0.011	0.005	0.011

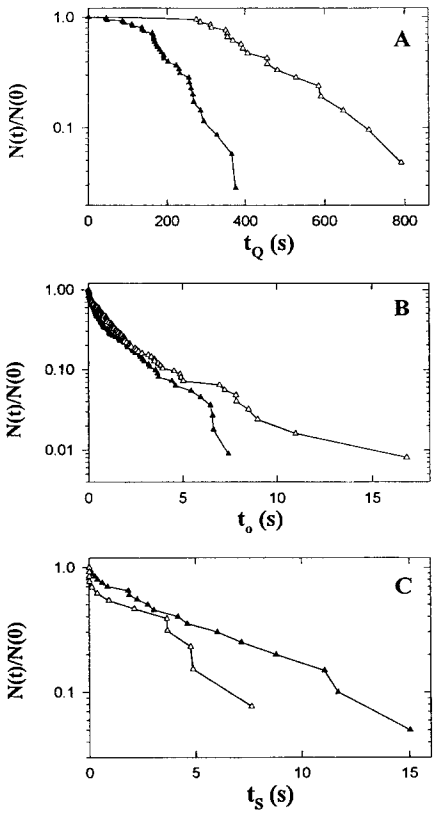

FIGURE 3. Varying the density of active HA by differential cleavage of HA0 of HAb2 cells. (*A*) t_Q distributions for cells with an extensive (E/U, *filled triangles*) and low (L/U, *open triangles*) fraction of HA0-cleavage. HA was activated by exposing cells to a low trypsin concentration for short (2.5 min, L/U) or long (12 min, E/U) times. (*B* and *C*) t_o and t_S distributions for these cells plotted as described in legend to Fig. 2. t_o and t_S distributions were identical ($p > 0.1$) for the two treatments. From Figs. 2 and 3, we conclude that the density of HA affects the kinetics of fusion but not the evolution of pores once they have formed.

cally equivalent for the two cell lines.[1] Thus, the lifetimes of the transient and successful fusion pores were not affected by the density of active HA.

We altered the density of active HA in another manner, by exposing cells to a low (1 μg/ml) concentration of trypsin at room temperature for varied times to differentially cleave HA0 to its fusion competent form (Clague et al., 1991). L/U HAb2 cells (2.5 min of low trypsin treatment) exhibited slower fusion kinetics—longer delays, t_D, and less steep final slopes, k_F (Fig. 3 *A*, *open triangles*; Table I)—than E/U HAb2 cells (low trypsin for 12 min) with its higher density of active HA (*filled triangles*).

The t_o distributions for E/U (Fig. 3 *B*, *filled triangles*) and L/U (*open triangles*) HAb2 cells, with their different active HA densities but identical cell surfaces, were virtually superimposable. Also, the distributions of open lifetimes of successful pores, t_S, (Fig. 3 *C*) were statistically identical. Thus, increasing the surface density

1. The *S* stages reported for Madin-Darby canine kidney (MDCK) cells infected with influenza fusing to planar bilayers (Melikyan et al., 1993*b*) were overestimated because Y_0 and Y_{dc} were contaminated by increases in planar bilayer conductance, G_m. After correcting for these nonspecific increases in G_m (see Materials and Methods), the waiting time distributions in the *S* stage for infected MDCK cells were similar to the transfected HAb2 cells.

of active HA clearly shortens the delay, and increases the rate of the limiting step of fusion pore opening, k_F. But the open times of transient and successful pores were independent of HA density.

Proteolytic Treatment of Cell Surface Affects Both the Waiting Time Until Fusion Pore Formation and the Open Times of Pores

Because cell surfaces contain integral and peripheral membrane proteins other than HA, we investigated how altering the cell surface proteins by proteolysis affected fusion. We treated HAb2 cells with a high concentration of chymotrypsin which would proteolyze cellular proteins but not activate HA0. Alternatively, be-

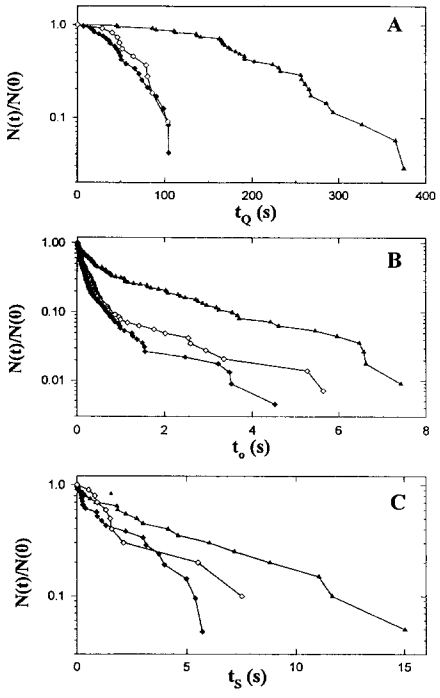

FIGURE 4. Properties of cell membranes affect kinetics of fusion and transient open pore lifetimes, but do not affect lifetimes of successful pores. *A–C* show t_Q, t_o, and t_S distributions, respectively, as described in legend to Fig. 2. HAb2 cells were treated with high concentrations of chymotrypsin (E/C, *filled diamonds*) or hyaluronidase/collagenase P (E/H, *open diamonds*). E/U (*filled triangles*) HAb2 cells shown previously (Fig. 4) are displayed once more for ease of comparison. (*B*) t_o distributions are identical for E/C and E/H cells ($p > 0.1$) and are statistically shorter than for E/U cells ($p < 0.001$). (*C*) In contrast, all the t_S distributions were identical ($p > 0.05$).

cause 3T3 cells secrete collagen and hyaluronic acid (Underhill and Toole, 1982) we incubated other batches of cells with collagenase P and hyaluronidase to remove the secreted cell coat. Control experiments using these cells did not lead to fusion, functionally verifying that chymotrypsin or hyaluronidase/collagenase did not activate HA0. These cells were then treated with a low concentration of trypsin for 12 min (protocols *c* and *d* of Materials and Methods) which activated an extensive amount of HA0. These E/C (Fig. 4 *A*, *closed diamonds*) and E/H (*open diamonds*) cells exhibited the same kinetics of fusion as judged by their virtually identical t_Q distributions. The t_Q distribution for E/U cells was also replotted (Fig. 5 *A*, *closed triangles*) to allow comparison, and the values of t_D and k_F were tabulated for the dif-

ferent treatments (Table I). It is clear that enzymatically treating cell surfaces leads to higher rates of fusion.

Whereas the density of active HA did not affect the open lifetimes of transient pores, altering cell surfaces by proteolytic treatment did shorten pore lifetimes. However, the degree of shortening depended on the precise enzymes used to treat the cells. Pores with untreated E/U cells had the longest open lifetimes (Fig. 4 *B*, *closed triangles*). E/C (*filled diamonds*) and E/H (*open diamonds*) HAb2 cells had identical t_o distributions. The lifetimes of pores from F/T cells (Fig. 2 *B*, *solid circles*) were shorter than for E/U cells, but longer than occurred with E/C and E/H cells. This order of pore lifetimes is the same as the order of kinetics of fusion: E/U slowest, F/T intermediate, to E/C and E/H fastest. Thus, fast fusion kinetics apparently correlates with short open pore lifetimes. In contrast, the duration of successful pores was independent of the type of proteolytic treatment, with all cells exhibiting statistically indistinguishable t_S distributions (Figs. 3 *C* and 4 *C*). For all HA densities and proteolytic treatments, t_S distributions were longer than the corresponding t_o distributions (Figs. 2–4).

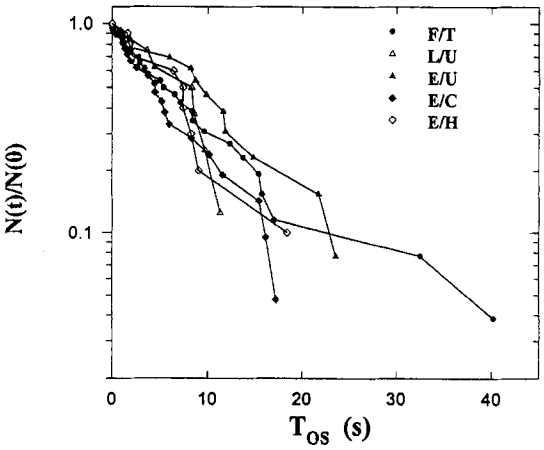

FIGURE 5. Distributions of total open times (T_{os}) for HAb2 cells. For each experiment, the total time fusion pores were open as both transient and successful pores before a pore entered the *T* stage (Fig. 1) was obtained. L/U (*open triangles*), F/T (*filled circles*), E/U (*filled triangles*), E/C (*filled diamonds*), and E/H (*open diamonds*). All these distributions were statistically identical ($p > 0.1$) and were reasonably well described by single exponentials (not shown).

The Total Open Lifetimes of Transient Open and Successful Pores Are Independent of Cell Surface Conditions and HA Density

For each membrane, the total open time, T_{os}, was determined as a sum of durations of the transient and successful openings before a pore fully enlarged (e.g., T_{os} is equal to the sum of lifetimes, t_o, for flickers 1 through 5, and the S stage pore, t_S, Fig. 1). All the waiting time distributions of T_{os} were reasonably well-fit by single exponentials ($0.94 < r^2 < 0.98$). The T_{os} distributions did not vary with cell treatments (Fig. 5). Neither the active HA density nor the cell surface treatment protocol appreciably affected them. Similarly, the waiting time distributions of the total time pores were open as flickering pores within the same experiment, T_o, were not significantly affected by the active HA density or the cell surface treatment (data

not shown). Thus T_{os}, T_o, and t_S (Figs. 2 *C*, 3 *C*, and 4 *C*) do not vary with either HA density or proteolytic treatment. As expected from the invariance of T_o, conditions leading to shorter open transient lifetimes correlated with a greater number of flickers. Only records containing pores that entered the *T* stage were used for this analysis. As reported above, when the surfaces of HAb2 cells were enzymatically treated, records always exhibited pores in the *T* stage. However, for untreated HAb2 cells and F/T GP4f cells, pores dilated into the *T* stage in only a fraction of the experiments. If a pore did not fully open, the duration of the *S* stage was undefined. Thus, T_{os} was indeterminate in the absence of full pore enlargement.[2]

Interflicker Intervals Depend on HA Density

The kinetics of transient pore formation within the repetitive flickering stage was analyzed from waiting time distributions of the interflicker intervals, t_i (Fig. 6), the time between consecutive openings. These distributions, obtained by pooling all fusion experiments for a given cell treatment protocol, could be reasonably described by a sum of two exponentials (not shown). Qualitatively, cells expressing lower densities of active HA (Fig. 6 *A*, *open symbols*) had longer times between openings than those with higher HA density (Figs. 6, *A* and *B*, *filled symbols* and *lines*). The protease used to treat cell surfaces also affected the t_i distributions. The times between flickers were shortest for E/C (Fig. 6 *B*, *solid line*) and E/H (*dashed line*) HAb2 cells. Basically, when varying cell surface treatment, slow kinetics of fusion, assessed by t_Q distributions, correlated with long interflicker intervals, long open times of transient pores, and low probability of fusion pores reaching the *T* stage.

Particularly long interflicker intervals (>40 s) are prominent for F/T GP4f, L/U HAb2, and E/U HAb2 cells with poor fusion activity. These very long interflicker intervals (Fig. 6 *A*) are possibly the times between termination of pore flickering in one cell and the beginning of activity in another. Flickering often occurred in bursts; open pores were interrupted by relatively brief closings and each burst was separated by long electrically silent periods. This bursting pattern may explain why at least two exponentials are required to fit the t_i distributions. For highly active cells (e.g., E/C and E/H HAb2 cells) the intervals between bursts were relatively short, as seen from the absence of long tails in their t_i distributions (Fig. 6 *B*, *solid* and *dashed lines*). In this interpretation, the "initial slopes" of the t_i distributions would reflect pore openings within bursts. To summarize, varying HA density and

2. L/U HAb2 cells showed more variability from day to day (i.e., from batch to batch) than others. For some batches, fusion into T stages usually occurred. For other batches, full enlargement was rare. For all cell types, without full enlargement, pores flickered for extended times. Inevitably, the planar membrane conductance, G_m, increased significantly after a few minutes of pore flickering, effectively terminating the ability to detect further flickering or opening to the *S* stage from increases in Y_0. Full pore enlargement to the *T* stage could, however, be observed from increases in Y_{90}. The t_o distribution (Figs. 2 *B* and 4 *B*) included all flickers, regardless of whether the *T* stage was reached. Limiting ourselves to analyzing T_{os} for membranes without appreciable G_m contamination and with pores that fully enlarged tended to eliminate experiments with pore activity that extended over prolonged periods of time. This was more prone to occur for cells with poor fusion activity; their values of T_{os} could be underestimated. The absence of complete pore dilation is probably related to the generally poor fusion activity of F/T GP4f and L/U HAb2 cells.

proteolytic treatment affects both indicators of fusion kinetics: the waiting time of fusion pores, t_Q, and the interflicker interval between pores, t_i. Faster kinetics correlates with shorter interflicker intervals.

The T_{os} and t_S distributions were generated only from experiments with complete fusion pore dilation, whereas t_o and t_i distributions included all transient flickering pores. It was possible that t_o and t_i distributions varied with treatment protocols but T_o and t_S distributions did not, simply because the distributions were derived from different sets of experiments. We, therefore, separately plotted t_i and t_o distributions of L/U HAb2 cells—where enlargement into the T stage was least frequent—for experiments in which complete pore dilation was (Fig. 7, *open circles*) or was not

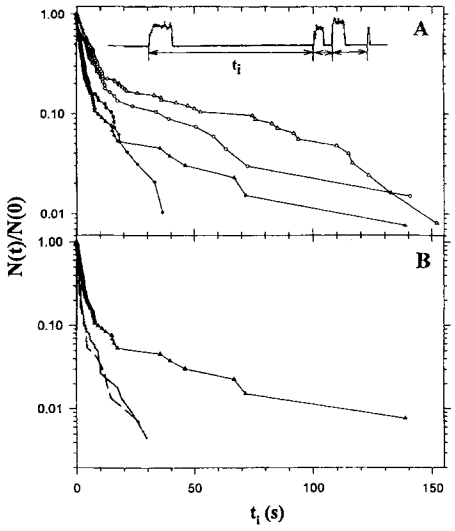

FIGURE 6. Waiting time distribution of intervals between initiation of transient fusion pore openings, t_i. (*A, top*) Three consecutive interflicker times, t_i, are illustrated for a typical experiment. (*Bottom*): t_i distributions are shown as a function of HA density: F/T HAb2 and GP4f cells (*filled and open circles*, respectively); E/U and L/U HAb2 cells (*filled and open triangles*). Because open times were short compared to closed times (t_c), $t_i \approx t_c$. (*B*) Proteolytic treatment shortens t_i: E/C HAb2 cells (*solid line*), E/H cells (*dotted line*), and E/U (*closed triangles*) cells. Multiple exponentials were required to fit the interflicker time intervals.

(*filled circles*) detected. Both t_i distributions (Fig. 7 *A*) were statistically identical; we conclude that interflicker intervals were the same for membranes that exhibited T stage pores as for membranes that did not. Open times of transient pores, however, were statistically shorter (Fig. 7 *B*) and t_Q was distributed over shorter times (data not shown) in experiments that exhibited a T stage. But the dissimilar t_o distributions for L/U HAb2 cells from experiments with and without T stages does not account for the difference in t_o between L/U HAb2 cells and other cells (Fig. 4 *B*). The t_o distribution of L/U cells with full pore enlargement (Fig. 7 *B, open circles*) was still statistically longer ($p < 0.05$) than for the other cells, treated with proteases. Thus, t_o distributions depended on treatment protocols, whether or not T stages were reached.

In summary, as expected, increasing the HA density resulted in faster fusion, characterized by shorter t_Q and t_i, and full opening of fusion pores. Whereas varying the density of HA did not affect t_o, speeding up fusion by altering the cell surface did lead to shorter t_o. Even for a cell treatment that did not guarantee full pore enlargement, shorter t_Q correlated with shorter t_o and a pore reaching the T stage.

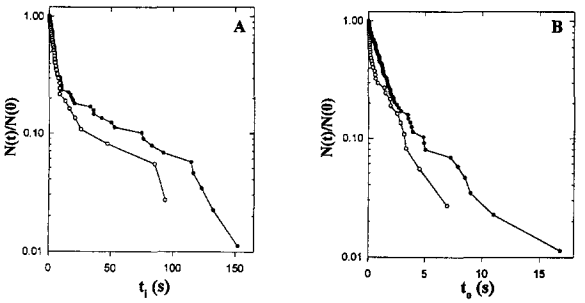

FIGURE 7. Fusion pore evolution for L/U HAb2 cells divided into experiments that exhibited (*open circles*) or did not exhibit (*filled circles*) complete pore dilation. (*A*) Interflicker intervals. The two distributions were identical ($p > 0.1$). (*B*) Open time distributions. The two distributions were not equivalent ($p < 0.05$).

DISCUSSION

Single vs Multiple Pore Flickering

Transient flicker events are common for the cell-bilayer system but not the rule for mast cell exocytotic secretion (Fernandez, Neher, and Gomperts, 1984; Zimmerberg, Curran, Cohen, Brodwick, 1987; Breckenridge and Almers, 1987; Oberhauser, Monck, and Fernandez, 1992; Alvarez de Toledo, Fernandez-Chacon, and Fernandez, 1993) and HA-mediated erythrocyte-fibroblast fusion (Spruce et al., 1989, 1991). Flickers are not observed for fusion between pairs of insect cells infected with Semliki Forest Virus, SFV, (Lanzrein, Käsermann, Weingart and Kempf, 1993) or baculovirus (Plonsky and Zimmerberg, 1994). However, the existence of pores that remain within a limited conductance range before final dilation is common. It occurs for fusion pores in mast cell secretion (Curran, Cohen, Chandler, Munson, and Zimmerberg, 1993) and virus fusion protein mediated cell–cell fusion. For these systems, fusion pores typically dilate fully.

It is not clear whether flickers are due to the same pore repetitively opening and closing or due to different pores, possibly from separate cells adhered to the planar bilayer. In exocytosis, the existence of numerous granules leads to analogous ambiguities: it is not clear that fully open pores derive from previous flickering ones or that they even arise from the same granules. Even in the absence of transient fusion events, it is difficult to distinguish, by electrical techniques, between enlargement of a single pore and sequential formation of several small fusion pores. For HA-expressing cell-erythrocyte fusion wherein single cell pairs are studied, it has been concluded from fluorescent dye measurements that incremental jumps in measured pore conductance occur by the formation of many small pores, creating a "colander" with large total conductance but small sieving diameters (Zimmerberg et al., 1994). Multiple fusion pores also probably formed between SFV- and baculovirus-infected insect cells (Lanzrein et al., 1993; Plonsky and Zimmerberg, 1994). These pores were irreversible.

We previously described pore enlargement in infected MDCK cell–planar bilayer fusion as if a single fusion pore migrated through several transient openings before irreversibly expanding into *S* and *T* stages (Melikyan et al., 1993*a,b*). The electrically quiescent stage from acidification to the first fusion pore, denoted the *Q* stage, was followed by repetitive flickering (called the *R* stage) before entering the *S* and *T* stages. While this approach formally describes pore evolution, there are concep-

tual problems with a single pore postulate. For example, in the simplest view, a fully configured single pore would contain the required complement of HAs and the interflicker intervals would be independent of the surrounding active HA density. But the time intervals between transient pore openings (Fig. 6) were shorter for cells with higher HA density: F/T HAb2 cells had shorter interflicker intervals than the lower HA-density F/T GP4f cells; E/U HAb2 had shorter interflicker intervals than did L/U HAb2 cells. On the other hand, increases in HA density would be expected to cause decreases in interflicker intervals if flickering were due to several transient openings of different pores because the HAs needed to form each pore would associate more quickly. But more complex views of a single structure giving rise to flickering could also account for the dependence of the t_i distribution on HA density. For example, multiple pores originating from a single intermediate but with a different number of HAs could be involved in each pore opening. Comparison of t_i distributions tacitly assumes that each flicker was due to a distinctly separate pore. Analyzing closed time intervals, t_c, would assume that each flicker was due to the same pore. Because open times were short compared to closed times, in practice it does not matter which of the distributions is analyzed because $t_i \approx t_c$.

Comparison of Cell-Bilayer Fusion Pores to Mast Cell Exocytotic Pores

Greater HA density sped the occurrence of pore openings (determined from t_Q and t_i distributions) but did not affect closings (obtained from t_o distributions). In contrast, the extent of cell surface proteolysis affected all three, t_Q, t_i, and t_o distributions. In mast cell exocytosis, it has been concluded that the rates of fusion pore openings and closings had different temperature dependencies (Oberhauser et al., 1992), and different relationships to intracellular concentrations of GTP and Ca^{2+} (Alvarez de Toledo and Fernandez, 1990). While the measured rates of fusion pore openings in the exocytotic system may reflect docking as well as fusion itself, it appears that, in general, different factors govern the energetics of pore openings and closings.

Open time distributions of flickering pores exhibit single exponentials in mast cell exocytosis (Oberhauser et al., 1992) whereas multiple exponential distributions are characteristic of fusion of HA-expressing cell lines (Figs. 2, 3, and 4, fits not shown) and of MDCK cells infected with influenza virus (Melikyan et al., 1993*b*) to planar membranes. Multiple exponentials may occur in the model system because the HA-presenting cells probably exhibit significant heterogeneity. When distributions are generated from individual experiments, the variations between batches of cells and between planar membranes are eliminated. While t_o distributions generated from individual experiments can be adequately fit by single exponentials, the small number of transient pores per experiment, typically 5–12, limits the power of this approach.

Proteolysis of HA-containing Cell Surfaces Affects Rates of Fusion

Clearing fibroblast surfaces of proteins not relevant to fusion leads to faster kinetics and higher competence of fusion to planar bilayers. Chymotrypsin and collagenase/hyaluronidase were equally capable of facilitating fusion (Fig. 5 A), both

more effective than trypsin. Apparently the high concentration of trypsin did not proteolyze the cell surfaces as effectively for fusion as the other proteases: F/T HAb2 cells had a somewhat higher density of active HA, but slower fusion kinetics, than E/C or E/H HAb2 cells. Chymotrypsin may be more effective because it is relatively nonspecific, cleaving peptide bonds that follow aromatic residues and, to a lesser degree, that follow other hydrophobic residues (Creighton, 1983). Collagenase and hyaluronidase are relatively specific for components of the extracellular matrix of 3T3 cells. Because a specific and nonspecfic enzyme equally promote fusion competence of cells, we presume that many enzymatic treatments could be used.

The membranes defining small fusion pores must be highly curved and therefore must store substantial membrane bending energy (Leikin, Kozlov, Chernomordik, Markin, and Chizmadzhev, 1987; Kozlov, Leikin, Chernomordik, Markin, and Chizmadzhev, 1989; Nanavati, Markin, Oberhauser, and Fernandez, 1992; Siegel 1993; Chizmadzhev, Cohen, Zimmerberg, and Scherbakov, 1994). This energy depends on many parameters—pore geometry, bending modulus, and intrinsic curvature of the membrane. The total energy associated with pores, due to bending and other factors (e.g., planar bilayer tension), will thus affect the rates of pore openings and closings. The nature of the cell surface, modified by proteolytic treatment, influences this energy. Also, proteins not directly involved in fusion may sterically interfere with intimate association between apposing membranes. Extensive proteolysis may relieve this interference, thereby promoting faster fusion.

Dynamics of Fusion Pores

Time courses of fusion have been obtained with populations of cells utilizing spread of R18 (or other fluorescent dyes) from erythrocytes to HA-expressing cells (Puri et al., 1990; Clague et al., 1991; Kaplan et al., 1991), or from virus to erythrocytes (Lowy, Sarkar, Chen, and Blumenthal, 1990; Puri et al., 1990). Kinetic schemes describing these time courses have been constructed (Blumenthal, Schoch, Puri, and Clague, 1991; Bentz, 1992). Generally, there are delay times from acidification to fusion (Clague et al., 1991). Our values of t_D are analogous to the delay times determined in these population studies. The presence of delays suggests that several steps are required for fusion. For a sequential state model, the final slopes of the t_Q distributions give the transition rate constant of the rate-limiting step; the number of non–rate-limiting steps and values of the transition rate constants determine the delay time. Delays are not universally observed, however. When the non–rate-limiting steps are sufficiently fast, waiting time distributions are single exponentials. Fusion with planar membranes of both the PR/8/34 strain of virus (Niles and Cohen, 1993) and cells infected with the same strain (Melikyan et al., 1993*b*) did not exhibit a delay. For PR/8/34, the kinetics of fusion can be therefore characterized by a single transition, two-state model. The slope of the single-exponential waiting time distribution for virus was more than an order of magnitude greater than that of infected cells. This is in accord with the finding that higher densities of HA lead to faster fusion. Within the context of a sequential state model, increasing either the density of active HA or the extent of proteolytic treatment speeds up both the rate-limiting and non-rate-limiting steps (Table I). However, the delays

were somewhat more sensitive to proteolytic treatment and to active HA density than were the final slopes, k_F (Table I), suggesting that either non–rate-limiting steps were the more affected or some steps were eliminated.

Our measurements indicate that the time course of pore evolution is fundamentally probabilistic. The energetics of the system, which is set by membrane mechanics, is needed to calculate transition rate constants. In the cell-planar membrane system, the rate constant for a pore to close must be about an order of magnitude higher than that for a pore to fully open to account for the multiple flickering events. Equivalently, an open pore is separated from a closed configuration by a smaller energy barrier than separates it from a fully enlarged one. Both shorter interflicker intervals and shorter openings with increased proteolytic treatments would result if the treatment lowered the energy barrier separating open pores from closed ones. The higher rate constant for closing predicts that transient pores should have shorter open lifetimes than successful pores in the semistable stage, as experimentally observed (Figs. 2–4). In fact, untreated cells had fewer flickers with longer lifetimes than did treated cells (Fig. 4 *B*). This predicts that t_o and t_S distributions should resemble each other more for untreated than for treated cells, as experimentally verified.

The constancy of T_{os} (Fig. 5) suggests that the barriers separating small open pores from the fully enlarged T stage pores were not affected by the density of HA or extent of cell surface proteolysis. Unaffected barriers make intuitive sense because the further the pore evolves from its initial state, the less it would be expected to depend on the fusion protein and conditions promoting fusion. To the extent that the T_{os} distribution can be described by a single exponential, a single large barrier hinders the full opening of the pore.

We conclude from this study that HA controls both rate-limiting and non–rate-limiting steps leading to fusion pore formation. Once pores are formed, however, their stability is independent of the density of the fusion protein. Rather, stability is controlled by general mechanical properties of merged membranes. The nature of conductance trajectories for pores that close and for pores that fully open are considered in the companion paper (Melikyan et al., 1995).

We thank Dr. Judith White for the gift of GP4f and HAb2 cells and sera against Japan/57 influenza virus. We are grateful to Barbara Newton and Dr. Mark Peeples for help with the immunoprecipitations and use of their facilities. Drs. Leonid Chernomordik and Joshua Zimmerberg read the manuscript and gave critical and constructive suggestions.

This work supported by National Institutes of Health GM 27367.

Original version received 21 November 1994 and accepted version received 1 June 1995.

REFERENCES

Alvarez de Toledo, G., and J. M. Fernandez. 1990. The effect of GTPγS and Ca^{++} on the kinetics of exocytosis of single secretory granules in peritoneal mast cells. *Biophysical Journal.* 57:495*a*. (Abstr.)

Alvarez de Toledo, G., R. Fernandez-Chacon, and J. M. Fernandez. 1993. Release of secretory products during transient vesicle fusion. *Nature.* 363:554–558.

Bentz, J. 1992. Intermediates and kinetics of membrane fusion. *Biophysical Journal.* 63:448–459.

Blumenthal, R., C. Schoch, A. Puri, and M. Clague. 1991. A dissection of steps leading to viral envelope protein-mediated membrane fusion. *Annals of the New York Academy of Sciences (Calcium Entry and Action at the Presynaptic Nerve Terminal).* 635:285–296.

Breckenridge, L. J., and W. Almers. 1987. Final steps in exocytosis observed in a cell with giant secretory granules. *Proceedings of the National Academy of Sciences.* 84:1945–1949.

Bullough, P. A., F. M. Hughson, J. J. Skehel, and D. C. Wiley. 1994. Structure of influenza haemagglutinin at the pH of membrane fusion. *Nature.* 371:37–43.

Chizmadzhev, Y. A., F. S. Cohen, J. Zimmerberg, and A. Scherbakov. 1994. Membrane mechanics can account for fusion pore dilation in stages. *Biophysical Journal.* 66:A283. (Abstr.)

Clague, M. J., C. Schoch, and R. Blumenthal. 1991. Delay time for influenza virus hemagglutinin-induced membrane fusion depends on hemagglutinin surface density. *Journal of Virology.* 65:2402–2407.

Creighton, T. E. 1983. Proteins. Structures and molecular principles. W. H. Freeman and Company, NY. 515 pp.

Curran, M., F. S. Cohen, D. E. Chandler, P. J. Munson, and J. Zimmerberg. 1993. Exocytotic fusion pores exhibit semi-stable states. *Journal of Membrane Biology.* 133:61–75.

Doms, R. W., A. Helenius, and J. M. White. 1985. Membrane fusion activity of the influenza virus hemagglutinin (the low pH-induced conformational change). *Journal of Biological Chemistry.* 260:2973–2981.

Doxsey, S. J., J. Sambrook, A. Helenius, and J. M. White. 1985. An efficient method for introducing macromolecules into living cells. *Journal of Cell Biology.* 101:19–27.

Doyle, C., M. G. Roth, J. Sambrook, and M.-J. Gething. 1985. Mutations in the cytoplasmic domain of the influenza virus hemagglutinin affects different stages of intracellular transport. *Journal of Cell Biology.* 100:704–714.

Ellens, H., S. Doxsey, J. S. Glenn, and J. M. White. 1989. Delivery of macromolecules into cells expressing a viral membrane fusion protein. *Methods in Cell Biology.* 31:155–176.

Ellens, H., J. Bentz, D. Mason, F. Zhang, and J. M. White. 1990. Fusion of influenza hemagglutinin-expressing fibroblasts with glycoprotein-bearing liposomes: role of hemagglutinin surface density. *Biochemistry.* 29:9697–9707.

Fernandez, J. M., E. Neher., and B. D. Gomperts. 1984. Capacitance measurements reveal stepwise fusion events in degranulating mast cells. *Nature.* 312:453–455.

Ferro-Novick, S., and R. Jahn. 1994. Vesicle fusion from yeast to man. *Nature.* 370:191–193.

Gething, M.-J., R. W. Doms, D. York, and J. M. White. 1986. Studies on the mechanism of membrane fusion: site-specific mutagenesis of the hemagglutinin of influenza virus. *Journal of Cell Biology.* 102: 11–23.

Godley, L., J. Pfeifer, D. Steinhauser, B. Ely, G. Shaw, R. Kaufmann, E. Suchanek, C. Pabo, J. J. Skehel, D. C. Wiley, and S. Wharton. 1992. Introduction of intersubunit disulfide bonds in the membrane-distal region of the influenza hemagglutinin abolishes membrane fusion activity. *Cell.* 68: 635–645.

Joshi, C., and J. M. Fernandez. 1988. Capacitance measurements. An analysis of the phase detector technique used to study exocytosis and endocytosis. *Biophysical Journal.* 53:885–892.

Kaplan, D., J. Zimmerberg, A. Puri, D. P. Sarkar, and R. Blumenthal. 1991. Single cell fusion events induced by influenza hemagglutinin: studies with rapid flow, quantitative fluorescence microscopy. *Experimental Cell Research.* 195:137–144.

Kemble, G. W., Y. I. Henis, J. M. White. 1993. GPI- and transmembrane-anchored influenza hemagglutinin differ in structure and receptor binding activity. *Journal of Cell Biology.* 122:1253–1265.

Kemble, G. W., T. Danieli, and J. M. White. 1994. Lipid-anchored influenza hemagglutinin promotes hemifusion, not complete fusion. *Cell.* 76:383–391.

Kozlov, M. M., S. L. Leikin, L. V. Chernomordik, V. S. Markin, and Y. A. Chizmadzhev. 1989. Stalk mechanism of membrane fusion. *European Biophysical Journal.* 17:121–129.

Lanzrein, M., N. Käsermann, R. Weingart, and C. Kempf. 1993. Early events of Semliki Forest virus-induced cell-cell fusion. *Virology.* 196:541–547.

Leikin, S. L., M. M. Kozlov, L. V. Chernomordik, V. S. Markin, and Y. A. Chizmadzhev. 1987. Membrane fusion overcoming of the hydration barrier and local restructuring. *Journal of Theoretical Biology.* 129:411–425.

Lindau, M., and E. Neher. 1988. Patch-clamp techniques for time-resolved capacitance measurements in single cells. *Pflügers Archiv.* 411:137–146.

Lowy, R. J., D. P. Sarkar, Y. Chen, and R. Blumenthal. 1990. Observation of single influenza virus-cell fusion and measurement by fluorescence video microscopy. *Proceedings of the National Academy of Sciences, USA.* 87:1850–1854.

Melikyan, G. B., W. D. Niles, M. E. Peeples, and F. S. Cohen. 1993*a*. Influenza hemagglutinin-mediated fusion pores connecting cells to planar membranes: flickering to final expansion. *Journal of General Physiology.* 102:1131–1149.

Melikyan, G. B., W. D. Niles, and F. S. Cohen. 1993*b*. Influenza virus hemagglutinin-iduced cell-planar bilayer fusion: quantitative dissection of fusion pore kinetics into stages. *Journal of General Physiology.* 102:1151–1170.

Melikyan, G. B., W. D. Niles, V. A. Ratinov, M. Karhanek, J. Zimmerberg, and F. S. Cohen. 1995. Comparison of flickering and successful fusion pores connecting influenza hemagglutinin expressing cells to planar membranes. *Journal of General Physiology.* 106:803–819.

Morris, S. J., D. P. Sarkar, J. M. White, and R. Blumenthal. 1989. Kinetics of pH-dependent fusion between 3T3 fibroblasts expressing influenza hemagglutinin and red blood cells. *Journal of Biological Chemistry.* 264:3972–3978.

Morrison, T., C. McQuain, and L. McGinnes. 1991. Complementation between avirulent Newcastle disease virus and a fusion protein gene expressed from a retrovirus vector: Requirements for membrane fusion. *Journal of Virology.* 65:813–822.

Nanavati, C., V. S. Markin, A. F. Oberhauser, and J. M. Fernandez. 1992. The exocytotic fusion pore modeled as a lipidic pore. *Biophysical Journal.* 63:1118–1132.

Niles, W. D., and F. S. Cohen. 1993. Single event recording shows that receptor docking alters the kinetics of membrane fusion mediated by influenza hemagglutinin. *Biophysical Journal.* 65:171–176.

Nobusawa, E., and K. Nakajima. 1988. Amino acid substitution at position 226 of the hemagglutinin molecule of influenza (H1N1) virus affects receptor binding activity but not fusion activity. *Virology.* 167:8–14.

Oberhauser, A., J. R. Monck, and J. M. Fernandez. 1992. Events leading to the opening and closing of the exocytotic fusion pore have markedly different temperature dependencies. *Biophysical Journal.* 61:800–809.

Plonsky, I., and J. Zimmerberg. 1994. Direct measurement of fusion pore conductance during virus-induced cell-cell fusion. *Biophysical Journal.* 66:A388. (Abstr.)

Puri, A., F. P. Booy, R. W. Doms, J. M. White, and R. Blumenthal. 1990. Conformational changes and fusion activity of influenza virus hemagglutinin of the H2 and H3 subtypes: Effects of acid pretreatment. *Journal of Virology.* 64:3824–3832.

Ruigrok, R. W. H., P. J. Andree, R. A. M. Hooft Van Huysduynen, and ?.?. Mellema. 1984. Characterization of three highly purified influenza virus strains by electron microscopy. *Journal of General Virology.* 65:799–802.

Sambrook, J., L. Rodgers, J. M. White, and M.-J. Gething. 1985. Lines of BPV-transformed murine cells that constitutively express influenza virus hemagglutinin. *EMBO Journal.* 4:91–103.

Sarkar, D. P., S. J. Morris, O. Eidelman, J. Zimmerberg, and R. Blumenthal. 1989. Initial stages of in-

fluenza hemagglutinin-induced cell fusion monitored simultaneously by two fluorescent events: cytoplasmic continuity and lipid mixing. *Journal of Cell Biology.* 109:113–122.

Siegel, D. P. 1993. Energetics of intermediates in membrane fusion: Comparison of stalk and inverted micellar intermediate mechanisms. *Biophysical Journal.* 65:2124–2140.

Skehel, J. J., P. M. Bayley, E. B. Brown, S. R. Martin, M. D. Waterfield, and J. M. White. 1982. Change in the conformation of influenza virus hemagglutinin at the pH optimum of virus-mediated membrane fusion. *Proceedings of the National Academy of Sciences, USA.* 79:968–972.

Söllner, T., and J. E. Rothman. 1994. Neurotransmission: Harnessing fusion machinery at the synapse. *Trends in Neurosciences.* 17:344–348.

Spruce, A. E., A. Iwata, J. M. White, and W. Almers. 1989. Patch clamp studies of single cell-fusion events mediated by a viral fusion protein. *Nature.* 342:555–558.

Spruce, A. E., A. Iwata, and W. Almers. 1991. The first milliseconds of the pore formed by a fusogenic viral envelope protein during membrane fusion. *Proceedings of the National Academy of Sciences.* 88: 3623–3627.

Stegmann, T., J. M. White, and A. Helenius. 1990. Intermediates in influenza induced membrane fusion. *EMBO Journal.* 9:4231–4241.

Suzuki, Y., Y. Nagao, H. Kato, M. Matsumoto, K. Nerome, K. Nakajima, and E. Nobusawa. 1986. Human influenza A virus hemagglutinin distinguishes sialyloligosaccharides in membrane-associated gangliosides as its receptor which mediates the adsorption and fusion process of virus infection. *Journal of Biological Chemistry.* 261:17057–17061.

Underhill, C. B., and B. P. Toole. 1982. Transformation-dependent loss of the hyaluronate-containing coats of cultured cells. *Journal of Cellular Physiology.* 110:123–128.

Van Meer, G., and K. Simons. 1983. An efficient method for introducing defined lipids into the plasma membrane of mammalian cells. *Journal of Cell Biology.* 97:1365–1374.

White, J. M. 1992. Membrane fusion. *Science.* 258:917–924.

White, J. M., and I. A. Wilson. 1987. Anti-peptide antibodies detect steps in a protein conformational change: low-pH activation of the influenza virus hemagglutinin. *Journal of Cell Biology.* 105:2887–2896.

White, J. M., A. Helenius, and M.-J. Gething. 1982. Haemagglutinin of influenza virus expressed from a cloned gene promotes membrane fusion. *Nature.* 300:658–659.

Wiley, D. C., and J. I. Skehel. 1987. The structure and function of the hemagglutinin membrane glycoprotein of influenza virus. *Annual Review of Biochemistry.* 56:365–394.

Wilson, I. A., J. J. Skehel, and D. C. Wiley. 1981. Structure of the haemagglutinin membrane glycoprotein of influenza virus at 3 Å resolution. *Nature.* 289:366–373.

Yewdell, J. W., W. Gerhard, and T. Bachi. 1983. Monoclonal anti-hemagglutinin antibodies detect irreversible antigenic alterations that coincide with the acid activation of influenza virus A/PR/8/34-mediated hemolysis. *Journal of Virology.* 48:239–248.

Zimmerberg, J., M. Curran, F. S. Cohen, and M. Brodwick. 1987. Simultaneous electrical and optical measurements show that membrane fusion precedes secretory granule swelling during exocytosis of beige mouse mast cells. *Proceedings of the National Academy of Sciences, USA.* 84:1585–1589.

Zimmerberg, J., S. S. Vogel, and L. V. Chernomordik. 1993. Mechanisms of membrane fusion. *Annual Review of Biophysics and Biomolecular Structure.* 22:433–466.

Zimmerberg, J., R. Blumenthal, D. P. Sarkar, M. Curran, and S. J. Morris. 1994. Restricted movement of lipid and aqueous dyes through the pore formed by influenza hemagglutinin during cell fusion. *Journal of Cell Biology.* 127:1885–1894.